

Magnetoelectric effects in heavy-fermion superconductors without inversion symmetry

Satoshi Fujimoto

Department of Physics, Kyoto University, Kyoto 606-8502, Japan

(Received 13 March 2005; published 12 July 2005)

We investigate the effects of strong electron correlation on magnetoelectric transport phenomena in noncentrosymmetric superconductors with particular emphasis on its application to the recently discovered heavy-fermion superconductor CePt₃Si. Taking into account electron correlation effects in a formally exact way, we obtain the expression of the magnetoelectric coefficient for the Zeeman-field-induced paramagnetic supercurrent, the existence of which was predicted more than a decade ago. It is found that in contrast to the usual Meissner current, which is much reduced by the mass renormalization factor in the heavy-fermion state, the paramagnetic supercurrent is not affected by the Fermi liquid effect. This result implies that the experimental observation of the magnetoelectric effect is more feasible in heavy-fermion systems than that in conventional metals with moderate effective mass.

DOI: [10.1103/PhysRevB.72.024515](https://doi.org/10.1103/PhysRevB.72.024515)

PACS number(s): 74.20.-z, 74.25.Fy, 74.70.Tx

I. INTRODUCTION

It has been discussed for decades that metallic systems with noncentrosymmetric crystal structure may exhibit nontrivial magnetoelectric effects.¹⁻⁵ The existence of an asymmetric potential gradient $\vec{\nabla}V$ due to the noncentrosymmetric structure gives rise to the spin-orbit interaction $(\vec{p} \times \vec{\nabla}V) \cdot \vec{\sigma}$, which breaks the individual inversion and spin rotation symmetry. As a result, the charge or energy current operator may couple to the spin-density operator. In this context, current flows induced by an applied magnetic field and current-flow-driven magnetization have been investigated extensively both in normal metals^{1,2} and superconductors.³⁻⁵ In particular, Edelstein predicted the remarkable magnetoelectric effect in superconducting states; i.e., in noncentrosymmetric superconductors, the Zeeman field induces a supercurrent, and conversely, the supercurrent flow induces a magnetization.^{3,4} Later, the former effect is elegantly reformulated by Yip in terms of the “van Vleck” contribution which stems from the inversion-symmetry-breaking spin-orbit interaction.⁵ Since a static magnetic field cannot induce dissipative current flows, the Zeeman-energy-induced current should vanish in the normal state. However, in the superconducting state, the existence of the paramagnetic supercurrent is not forbidden in the absence of the inversion symmetry. The recent discovery of superconducting materials without inversion symmetry such as CePt₃Si, UIr, and Cd₂Re₂O₇ stimulates the renewed interest in this issue.⁶⁻¹² Under an applied magnetic field, the Meissner diamagnetic supercurrent in addition to the Zeeman-field-induced paramagnetic supercurrent should exist. Thus, it is important for the experimental observation of this effect to discriminate between these two supercurrents.

In the present paper, we would like to investigate the Fermi liquid corrections to this Edelstein magnetoelectric effect, which may be important for the application to heavy-fermion superconductors such as CePt₃Si and UIr. We obtain the formula for the magnetoelectric effect coefficient taking into account Fermi liquid corrections exactly. The most important finding is that the Zeeman-energy-induced paramagnetic supercurrent is not at all affected by electron correla-

tion effects provided that ferromagnetic spin fluctuation is not developed, in contrast with the diamagnetic Meissner current of which the magnitude is much reduced by the mass renormalization effect. This result implies that the experimental detection of the paramagnetic supercurrent in heavy-fermion superconductors may be more feasible than that in weakly correlated metals.

The organization of this paper is as follows. In Sec. II, we present the basic formulation of the Fermi liquid theory for a model system without inversion symmetry. We would like to make a brief comment on the superconducting state realized in CePt₃Si in Sec. III. In Sec. IV, the exact formula of the magnetoelectric coefficient is obtained. In Sec. V, the implication for the experimental observation of this effect is discussed. Summary and discussion are given in the last section.

II. MODEL AND ANALYSIS BASED ON THE FERMI LIQUID THEORY

As a simplest model which realizes the broken inversion symmetry, we consider an interacting electron system with the Rashba spin-orbit interaction.¹³ The Hamiltonian is given by

$$\mathcal{H} = \sum_{p,\sigma} \varepsilon_p c_{\sigma p}^\dagger c_{\sigma p} + \alpha \sum_{p,\sigma\sigma'} (\vec{p} \times \vec{n}) \cdot \vec{\sigma}_{\sigma\sigma'} c_{\sigma p}^\dagger c_{\sigma' p} + U \sum_i n_{\uparrow i} n_{\downarrow i}, \quad (1)$$

where $c_{\sigma p}^\dagger$ ($c_{\sigma p}$) is the creation (annihilation) operator for an electron with spin σ and momentum p . The number density operator at the site i , $n_{\sigma i} = c_{\sigma i}^\dagger c_{\sigma i}$. The second term of Eq. (1) is the Rashba spin-orbit interaction which incorporates the broken inversion symmetry. Here, the unit vector parallel to the asymmetric potential gradient is given by $\vec{n} = (0, 0, 1)$. This system is considered to be a model of CePt₃Si, with which we are mainly concerned in this paper. The f electron of CePt₃Si is in the Γ_7 Kramers doublet state.¹¹ Expanding the Γ_7 doublet in terms of the $s_z = 1/2$ and $-1/2$ basis, we found that the Rashba spin-orbit interaction term expressed in term of the Γ_7 basis has the matrix structure given above

up to a constant factor which can be absorbed into the redefinition of the coupling constant α . Thus, in the case of CePt₃Si, the spin index σ in Eq. (1) represents the Γ_7 Kramers doublet. According to the LDA band calculations,^{10,30} the electronic structure near the Fermi level in CePt₃Si is predominated by the f -electron component. Since the leading interaction between f electrons is an on-site Coulomb type, we assume the interaction term as given by Eq. (1) for simplicity.

In the following, we do not specify the pairing mechanism of superconductivity, but assume that the superconducting state is realized by an effective pairing interaction with an angular momentum $l \geq 1$ which may stem from the on-site Coulomb interaction in Eq. (1) or may have any other origin not included in the Hamiltonian (1). Then, we can analyze electron correlation effects on this superconducting state in a formally exact way by using the superconducting Fermi liquid theory.¹⁴⁻¹⁶

In the conventional Nambu representation,¹⁷ the inverse of the single-particle Green's function is defined as

$$\hat{G}^{-1}(p) = \begin{pmatrix} i\varepsilon_n - \hat{H}(p) & -\hat{\Delta}(p) \\ -\hat{\Delta}^\dagger(p) & i\varepsilon_n + \hat{H}^\dagger(-p) \end{pmatrix}, \quad (2)$$

where $p = (\vec{p}, i\varepsilon)$, and

$$\hat{H}(p) = \hat{H}_0(p) + \hat{\Sigma}(p), \quad (3)$$

$$\hat{H}_0 = \varepsilon_p - \mu + \alpha(\vec{p} \times \vec{n}) \cdot \vec{\sigma} - \mu_B \sigma_x H_x, \quad (4)$$

with μ the chemical potential. Here, to discuss the magnetoelectric effect, we take into account the Zeeman magnetic field in the x direction, H_x . For simplicity, we assume that the g value is equal to 2. The self-energy matrix $\hat{\Sigma}$ consists of both diagonal and off-diagonal components,

$$\hat{\Sigma} = \begin{pmatrix} \Sigma_{\uparrow\uparrow}(p) & \Sigma_{\uparrow\downarrow}(p) \\ \Sigma_{\downarrow\uparrow}(p) & \Sigma_{\downarrow\downarrow}(p) \end{pmatrix}. \quad (5)$$

We can easily see from the symmetry argument that under the applied in-plane magnetic field, $\Sigma_{\uparrow\uparrow}(p) = \Sigma_{\downarrow\downarrow}(p) \equiv \Sigma(p)$ and $\Sigma_{\uparrow\downarrow}(\vec{p}, i\varepsilon) = \Sigma_{\downarrow\uparrow}^*(\vec{p}, -i\varepsilon)$. The superconducting gap function is $\{\hat{\Delta}(p)\}_{\alpha\beta} = \Delta_{\alpha\beta}(p)$ ($\alpha, \beta = \uparrow, \downarrow$).

$i\varepsilon_n - \hat{H}(p)$ and $i\varepsilon_n + \hat{H}^\dagger(-p)$ in $\hat{G}^{-1}(p)$ are diagonalized by the unitary transformation $\hat{A}(p)\hat{G}^{-1}(p)\hat{A}^\dagger(p)$ with

$$\hat{A}(p) = \begin{pmatrix} \hat{U}(\vec{p}) & 0 \\ 0 & \hat{U}^\dagger(-\vec{p}) \end{pmatrix}, \quad (6)$$

$$\hat{U}(\vec{p}) = \frac{1}{\sqrt{2}} \begin{pmatrix} 1 & i\hat{t}_- \\ i\hat{t}_+ & 1 \end{pmatrix}, \quad (7)$$

where $\hat{t}_\pm = \hat{t}_x \pm i\hat{t}_y$, and \hat{t}_x and \hat{t}_y are, respectively, the x and y components of the unit vector $\hat{t}_p \equiv \vec{t}_p / |\vec{t}_p|$ with

$$\vec{t}_p(i\varepsilon) = \left(p_x + \frac{1}{\alpha} \text{Im} \Sigma_{\uparrow\downarrow}(p_y) + \frac{1}{\alpha} \text{Re} \Sigma_{\uparrow\downarrow} - \frac{\mu_B H_x}{\alpha}, 0 \right). \quad (8)$$

As seen from Eqs. (3)–(5), the main effect of the off-diagonal self-energy $\Sigma_{\uparrow\downarrow}$ is to renormalize the Rashba interaction term, replacing the momentum \vec{p} in the Rashba term with the vector \vec{t}_p . Since the on-site Coulomb interaction does not change the symmetry of the system, the off-diagonal self-energy should satisfy the following condition in the absence of magnetic fields:

$$\text{Re} \Sigma_{\uparrow\downarrow}(p_x, -p_y) = -\text{Re} \Sigma_{\uparrow\downarrow}(p_x, p_y), \quad (9)$$

$$\text{Im} \Sigma_{\uparrow\downarrow}(-p_x, p_y) = -\text{Im} \Sigma_{\uparrow\downarrow}(p_x, p_y), \quad (10)$$

and $\text{Re} \Sigma_{\uparrow\downarrow}$ ($\text{Im} \Sigma_{\uparrow\downarrow}$) is an even function of p_x (p_y).

In the normal state, the single-particle excitation energy $\varepsilon_{p\tau}^*$ for the quasiparticle with the helicity $\tau = \pm 1$ is given by the solution of the equation $z - \hat{H}(\vec{p}, z) = 0$, which is, in the diagonalized representation,

$$\varepsilon_{p\tau}^* + \mu - \varepsilon_p - \tau \alpha |\vec{t}_p(\varepsilon_{p\tau}^*)| - \text{Re} \Sigma(\vec{p}, \varepsilon_{p\tau}^*) = 0. \quad (11)$$

The gap functions $\hat{\Delta}(p)$ and $\hat{\Delta}^\dagger(p)$ in $\hat{G}^{-1}(p)$ are also diagonalized by the unitary transformation $\hat{A}(p)\hat{G}^{-1}(p)\hat{A}^\dagger(p)$ provided that the gap function has the following structure:

$$\hat{\Delta}(p) = \Delta_s(p) i\sigma_y + \Delta_t(p) (\vec{t}_p \times \vec{n}) \cdot \vec{\sigma} i\sigma_y. \quad (12)$$

Here $\Delta_s(p)$ and $\Delta_t(p)$ are even functions of momentum \vec{p} . This means that the spin singlet and triplet component is mixed in the diagonalized basis labeled by $\tau = \pm 1$, and the \vec{d} vector of the triplet component is $\vec{t}_p \times \vec{n}$.^{3,18} In the case that $\hat{\Delta}(p)$ is not expressed as Eq. (12), $\hat{H}(p)$ and $\hat{\Delta}(p)$ cannot be diagonalized simultaneously, and the nonzero off-diagonal components of $\hat{\Delta}(p)$ which correspond to the Cooper pairing between the different Fermi surfaces induce pair-breaking effects, resulting in the decrease of the transition temperature T_c . Thus, the highest transition temperature is achieved by the gap function given by Eq. (12).¹⁹ The realization of the gap function (12) in the case with no inversion center is also elucidated by the group theoretical argument.²⁰

Taking the inverse of Eq. (2), we have

$$\hat{G}(p) = \begin{pmatrix} \hat{G}(p) & \hat{F}(p) \\ \hat{F}^\dagger(p) & -\hat{G}^\dagger(-p) \end{pmatrix}, \quad (13)$$

where

$$\hat{G}(p) = \sum_{\tau=\pm 1} \frac{1 + \tau(\vec{t}_p \times \vec{n}) \cdot \vec{\sigma}}{2} G_\tau(p), \quad (14)$$

$$\hat{F}(p) = \sum_{\tau=\pm 1} \frac{1 + \tau(\vec{t}_p \times \vec{n}) \cdot \vec{\sigma}}{2} i\sigma_y F_\tau(p), \quad (15)$$

and

$$G_\tau(p) = \frac{z_{p\tau}(i\varepsilon + \varepsilon_{p\tau}^*)}{(i\varepsilon + i\gamma \text{sgn } \varepsilon)^2 - E_{p\tau}^2}, \quad (16)$$

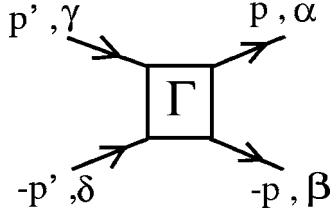


FIG. 1. Four-point vertex in the particle-particle channel.

$$F_{\tau}(p) = \frac{z_{p\tau}\Delta_{\tau}(p)}{(i\varepsilon + i\gamma \operatorname{sgn} \varepsilon)^2 - E_{p\tau}^2}. \quad (17)$$

Here the mass renormalization factor is

$$z_{p\tau} = \left[1 - \frac{\partial \operatorname{Re} \Sigma(p)}{\partial(i\varepsilon)} + \tau \left(\hat{t}_x \frac{\partial \operatorname{Im} \Sigma_{\uparrow\downarrow}(p)}{\partial(i\varepsilon)} + \hat{t}_y \frac{\partial \operatorname{Re} \Sigma_{\uparrow\downarrow}(p)}{\partial(i\varepsilon)} \right) \right]^{-1} \Bigg|_{i\varepsilon=E_{p\tau}}, \quad (18)$$

and γ is the quasiparticle damping. The single-particle excitation energy is $E_{p\tau} = \sqrt{\varepsilon_{p\tau}^{*2} + \Delta_{\tau}^2(p)}$ with $\Delta_{p\tau} = z_{p\tau}[\Delta_s(p) + \tau\Delta_t(p)]$.

The superconducting gap function $\Delta_{\alpha\beta}$ and the transition temperature are determined by the self-consistent gap equation,

$$\Delta_{\alpha\beta} = T \sum_{n,p} \operatorname{Tr}[\hat{\Gamma}^{\alpha\beta}(p,p')\hat{F}(p')], \quad (19)$$

where we have introduced the four-point vertex function matrix $\{\hat{\Gamma}^{\alpha\beta}(p,p')\}_{\gamma\delta}$ which is diagrammatically expressed as shown in Fig. 1. We expand the four-point vertex in the particle-particle channel $\{\hat{\Gamma}^{\alpha\beta}(p,p')\}_{\gamma\delta}$ in terms of the basis of the irreducible representations of the point group, and consider a component $\{\hat{\Gamma}_a^{\alpha\beta}(p,p')\}_{\gamma\delta}$ which corresponds to the pairing state giving the highest T_c . This pairing interaction consists of the spin singlet and triplet channel,

$$\{\hat{\Gamma}_a^{\alpha\beta}(p,p')\}_{\gamma\delta} = \Gamma_s(p,p')i(\sigma_y)_{\alpha\beta}i(\sigma_y)_{\gamma\delta} + \Gamma_t(p,p')(\hat{t}_p \times \vec{n}) \cdot (\vec{\sigma}i\sigma_y)_{\alpha\beta}(\hat{t}_{p'} \times \vec{n}) \cdot (\vec{\sigma}i\sigma_y)_{\gamma\delta}. \quad (20)$$

The symmetries of $\Gamma_s(p,p')$ and $\Gamma_t(p,p')$ in the momentum space are characterized by the same irreducible representation, and as a result, $\Delta_s(p)$ and $\Delta_t(p)$ in Eq. (12) have the same symmetry in the momentum space. The realized superconducting state is the mixture of the spin singlet and triplet states.^{3,18} In this case, the possible pairing state is $s+p$ or $d+f$ or $g+h$, and so forth.

III. A COMMENT ON THE SUPERCONDUCTING STATE REALIZED IN CePt₃Si: THE POSSIBILITY OF AN UNUSUAL COHERENCE EFFECT

Here, we would like to make a brief remark about the pairing state realized in CePt₃Si. The NMR measurement carried out by Yogi *et al.* shows the existence of the coherence peak of $1/T_1T$ just below T_c , indicating the full-gap

state without nodes.¹² On the other hand, the recent experiment on the thermal transport done by Izawa *et al.* supports the existence of line nodes of the superconducting gap.²³ A possible resolution of this discrepancy is that the line nodes of the superconducting gap are generated accidentally at the magnetic zone boundary which emerges as a result of the antiferromagnetic phase transition at $T_N=2.2$ K, and crosses the Fermi surface. For such accidental nodes without the sign change of the superconducting gap function, the coherence factor of $1/T_1T$ does not vanish, resulting in the enhancement of the coherence peak just below T_c . In this case, a plausible candidate for the pairing state is the $s+p$ wave state. An important point which we would like to stress here is that even when the superconducting state is dominated by the p wave pairing, i.e., $\Delta_s(p) \ll \Delta_t(p)$, the coherence factor which enters into $1/T_1T$ does not vanish. This contrasts with the case of the usual p wave state realized in centrosymmetric superconductors, where the coherence factor of $1/T_1T$ disappears. This is understood as follows. For simplicity, we ignore electron correlation effects. Then, in noncentrosymmetric superconductors, the nuclear relaxation rate is given by¹⁷

$$\begin{aligned} \frac{1}{T_1T} &\propto \lim_{\omega \rightarrow 0} \frac{1}{\omega} \operatorname{Im} \left(T \sum_{\varepsilon_m} \sum_{p,p'} \left\{ \operatorname{Tr} \left[\frac{\sigma^+}{2} \hat{G}(p, \varepsilon_m) \right. \right. \right. \\ &\quad \left. \left. \left. + \omega_n \frac{\sigma^-}{2} \hat{G}(p', \varepsilon_m) \right] - \operatorname{Tr} \left[\frac{\sigma^+}{2} \hat{F}(p, \varepsilon_m) \right. \right. \right. \\ &\quad \left. \left. \left. + \omega_n \frac{\sigma^-}{2} \hat{F}(p', \varepsilon_m) \right] \right\} \Bigg|_{i\omega_n \rightarrow \omega + i\delta} \right) \\ &= \int \frac{d\varepsilon}{2\pi} \frac{1}{2T \cosh^2 \frac{\varepsilon}{2T}} \{ [N_n(\varepsilon)]^2 + [N_a(\varepsilon)]^2 \}, \quad (21) \end{aligned}$$

with $N_n(\varepsilon)$ and $N_a(\varepsilon)$ defined by the retarded Green's functions as

$$N_n(\varepsilon) = - \sum_p \sum_{\tau=\pm} \operatorname{Im} G_{\tau}^R(p, \varepsilon), \quad (22)$$

$$N_a(\varepsilon) = - \sum_p \sum_{\tau=\pm} \operatorname{Im} F_{\tau}^R(p, \varepsilon). \quad (23)$$

The expression of $1/T_1T$ (21) does not rely on the phase factor $\hat{t}_p \times \vec{n}$ of the triplet component of the gap function (12). The second term on the right-hand side of Eq. (21) gives the nonzero contribution from the coherence factor, as in the case of conventional s -wave superconductors. This property enhances the coherence peak of $1/T_1T$ prominently. It may be important to take into account this unusual coherence effect for clarification of the origin of the notable coherence peak of $1/T_1T$ in CePt₃Si.¹² It is also intriguing to explore the unusual coherence effect on other response functions, such as the ultrasonic attenuation. We would like to address this issue elsewhere.

IV. MANY-BODY EFFECTS ON THE MAGNETOELECTRIC TRANSPORT IN THE SUPERCONDUCTING STATE

In this section, we consider electron correlation effects on the magnetoelectric transport in the superconducting state first found by Edelstein and later discussed in detail by Yip i.e., the emergence of the paramagnetic supercurrent induced by the Zeeman magnetic field in the direction normal to the \vec{n} vector.^{3,5}

We consider the charge current flowing in the y direction, which is defined as

$$J_y = T \sum_{\varepsilon, n, p} \frac{1}{2} \text{Tr}[\hat{V}_{0y} \mathcal{G}(p)] \quad (24)$$

with

$$\hat{V}_{0y} = \begin{pmatrix} \hat{v}_{0y}(\vec{p}) & 0 \\ 0 & -\hat{v}_{0y}^t(-\vec{p}) \end{pmatrix} \quad (25)$$

and $\hat{v}_{0y} = \partial_{p_y} \varepsilon_p + \alpha(\vec{n} \times \vec{\sigma})$.

The transport coefficient which characterizes Edelstein's magnetoelectric effect is given by

$$\begin{aligned} \mathcal{K}_{yx} &\equiv \left. \frac{\partial J_y}{\partial H_x} \right|_{H_x=0} \\ &= -T \sum_{n, p} \frac{1}{2} \text{Tr} \left[\hat{V}_{0y} \mathcal{G}(p) \frac{\partial \mathcal{G}^{-1}(p)}{\partial H_x} \mathcal{G}(p) \right] \Bigg|_{H_x=0}. \end{aligned} \quad (26)$$

Following Ref. 3, to simplify the expression of \mathcal{K}_{yx} we use Ward's identity for the current vertex,

$$\frac{\partial \hat{G}(p)}{\partial p_y} = \hat{G}(p) \hat{V}_y(\vec{p}) \hat{G}(p) + \hat{F}(p) \hat{V}_y^t(-\vec{p}) \hat{F}^\dagger(\vec{p}, -i\varepsilon) + \hat{R}(p), \quad (27)$$

where $\hat{V}_y(\vec{p}) = \hat{v}_{0y} + \partial \hat{\Sigma}(p) / \partial p_y$, and

$$\hat{R}(p) = \begin{pmatrix} 0 & r(p) \\ r^*(\vec{p}, -i\varepsilon) & 0 \end{pmatrix}, \quad (28)$$

$$r(p) = \left[\frac{G_+ - G_-}{2\alpha|\vec{r}_p|} - G_+ G_- + F_+ F_- \right] \hat{t}_+ \Lambda_{+-}^{cy}(p), \quad (29)$$

$$\Lambda_{+-}^{cy}(p) = \hat{t}_x \left(\alpha + \frac{\partial \text{Re} \Sigma_{\uparrow\downarrow}}{\partial p_y} \right) - \hat{t}_y \frac{\partial \text{Im} \Sigma_{\uparrow\downarrow}}{\partial p_y}. \quad (30)$$

Then, from Eqs. (13), (26), and (27), we obtain

$$\begin{aligned} \mathcal{K}_{yx} &= -2T \sum_{n, p} \text{Tr} \left[\hat{F}(p) \hat{v}_{0y}^t(-\vec{p}) \hat{F}^\dagger(p) \left(\mu_B \sigma_x - \frac{\partial \hat{\Sigma}}{\partial H_x} \right) \right] \\ &\quad - 2\mu_B \alpha T \sum_{n, p} F_+ F_- \hat{t}_x \Lambda_{+-}^{sx}(p) + T \sum_{n, p} \text{Tr} \left[\frac{\partial \hat{\Sigma}}{\partial p_y} \frac{\partial \hat{G}}{\partial H_x} \right] \\ &\quad - T \sum_{n, p} \text{Tr} \left[\frac{\partial \hat{\Sigma}}{\partial H_x} \frac{\partial \hat{G}}{\partial p_y} \right], \end{aligned} \quad (31)$$

where the three-point vertex function is

$$\Lambda_{+-}^{sx}(p) = \hat{t}_x \left(1 - \frac{1}{\mu_B} \frac{\partial \text{Re} \Sigma_{\uparrow\downarrow}}{\partial H_x} \right) + \frac{\hat{t}_y}{\mu_B} \frac{\partial \text{Im} \Sigma_{\uparrow\downarrow}}{\partial H_x}. \quad (32)$$

The last two terms of Eq. (31), which emerge as a result of Fermi liquid corrections, can be rewritten by using Luttinger-Ward's identity generalized to the superconducting state. Luttinger-Ward's identity in the normal state reads^{21,22}

$$T \sum_{n, p} \text{Tr} \left[\hat{\Sigma} \frac{\partial \hat{G}}{\partial p_\mu} \right] = 0. \quad (33)$$

This relation is obtained by differentiating all closed linked diagrams with respect to p_μ .^{21,22} In the superconducting state, a similar analysis leads to

$$\begin{aligned} T \sum_{n, p} \text{Tr} \left[\hat{\Sigma} \frac{\partial \hat{G}}{\partial p_\mu} \right] + T \sum_{n, p} \text{Tr} \left[\hat{\Delta}^\dagger \frac{\partial \hat{F}}{\partial p_\mu} \right] + T \sum_{n, p} \text{Tr} \left[\hat{\Delta} \frac{\partial \hat{F}^\dagger}{\partial p_\mu} \right] \\ = 0. \end{aligned} \quad (34)$$

Differentiating Eq. (34) with respect to H_x , and integrating over p_y by parts, we have

$$\begin{aligned} T \sum_{n, p} \text{Tr} \left[\frac{\partial \hat{\Sigma}}{\partial p_y} \frac{\partial \hat{G}}{\partial H_x} \right] - T \sum_{n, p} \text{Tr} \left[\frac{\partial \hat{\Sigma}}{\partial H_x} \frac{\partial \hat{G}}{\partial p_y} \right] \\ = -T \sum_{n, p} \text{Tr} \left[\frac{\partial \hat{\Delta}^\dagger}{\partial p_y} \frac{\partial \hat{F}}{\partial H_x} \right] + T \sum_{n, p} \text{Tr} \left[\frac{\partial \hat{\Delta}^\dagger}{\partial H_x} \frac{\partial \hat{F}}{\partial p_y} \right] \\ - T \sum_{n, p} \text{Tr} \left[\frac{\partial \hat{\Delta}}{\partial p_y} \frac{\partial \hat{F}^\dagger}{\partial H_x} \right] + T \sum_{n, p} \text{Tr} \left[\frac{\partial \hat{\Delta}}{\partial H_x} \frac{\partial \hat{F}^\dagger}{\partial p_y} \right]. \end{aligned} \quad (35)$$

We see from Eqs. (37) and (35) that \mathcal{K}_{yx} vanishes exactly in the normal state, as is consistent with the thermodynamic argument that a static magnetic field cannot induce nonequilibrium current flows.^{3,5} The right-hand side of Eq. (35) consists of the terms which have the form $\sum_{n, p} G_\tau F_{\tau'}$. The ratio of the contributions from these terms to those from other terms of Eq. (31) is of order Δ/E_F , and thus we can neglect the last two terms of Eq. (31) approximately. Then, the magnetoelectric coefficient is expressed as

$$\begin{aligned} \frac{\mathcal{K}_{yx}}{e\mu_B} = & \sum_p \sum_{\tau=\pm 1} \tau v_{0y\tau} \frac{z_{p\tau}^2 \Lambda_{p\tau}^2}{E_{p\tau}^2} \left[\frac{\text{ch}^{-2} \frac{E_{p\tau}}{2T}}{2T} - \frac{\text{th} \frac{E_{p\tau}}{2T}}{E_{p\tau}} \right] \Lambda_{\tau}^{sx}(p) \\ & + 2\alpha \sum_p \frac{z_{p+} z_{p-} \Delta_{p+} \Delta_{p-}}{E_{p+}^2 - E_{p-}^2} \left[\frac{\text{th} \frac{E_{p+}}{2T}}{E_{p+}} - \frac{\text{th} \frac{E_{p-}}{2T}}{E_{p-}} \right] \hat{t}_x \Lambda_{+-}^{sx}(p), \end{aligned} \quad (36)$$

where

$$\Lambda_{\tau}^{sx}(p) = \hat{t}_y \left(1 - \frac{1}{\mu_B} \frac{\partial \text{Re} \Sigma_{\uparrow\downarrow}}{\partial H_x} \right) - \frac{\hat{t}_x}{\mu_B} \frac{\partial \text{Im} \Sigma_{\uparrow\downarrow}}{\partial H_x} - \frac{\tau}{\mu_B} \frac{\partial \text{Re} \Sigma}{\partial H_x}. \quad (37)$$

It is noted that the vertex corrections due to electron correlation, $\Lambda^{sx}(p)$, which appear in the above expression (36) is nothing but the vertex corrections to the uniform spin susceptibility,

$$\begin{aligned} \chi_{xx} = & \mu_B^2 \sum_p \sum_{\tau=\pm 1} \frac{z_{p\tau}}{2E_{p\tau}^2} \left[\frac{\varepsilon_{p\tau}^{*2} \text{ch}^{-2} \frac{E_{p\tau}}{2T}}{2T} - \frac{\Delta_{p\tau}^2 \text{th} \frac{E_{p\tau}}{2T}}{E_{p\tau}} \right] \hat{t}_y \Lambda_{\tau}^{sx}(p) \\ & + \mu_B^2 \sum_p \left[\frac{\varepsilon_{p+}^* \text{th} \frac{E_{p+}}{2T}}{2E_{p+}} - \frac{\varepsilon_{p-}^* \text{th} \frac{E_{p-}}{2T}}{2E_{p-}} \right] \frac{\hat{t}_x}{\alpha |\hat{t}_p|} \Lambda_{+-}^{sx}(p). \end{aligned} \quad (38)$$

Equation (38) is easily obtained by differentiating the x component of the total magnetization $S^x = \mu_B T \sum_{n,p} \text{Tr}[\sigma_x \hat{G}(p)]$ with respect to H_x . Note that the first term on the right-hand side of Eq. (38) is the Pauli paramagnetic contribution and the second one is the ‘‘van Vleck’’ term which arises from excitations between spin-orbit split two bands. Generally, in heavy-fermion systems, the magnitude of the uniform spin susceptibility is enhanced by the vertex corrections $\Lambda^{sx}(p)$. In typical heavy-fermion systems including CePt₃Si, the Wilson ratio $R_W = T\chi/C/(T\chi_0/C_0) \sim 2$, which implies that the vertex corrections Λ^{sx} is approximately of order the mass enhancement factor $1/z_{p\tau}$.⁹ Therefore, in Eq. (36), effects of the vertex corrections and the mass renormalization factors $z_{p\tau}$ cancel with each other. This cancellation holds as long as there is no strong ferromagnetic spin fluctuation which increases notably the magnitudes of the vertex corrections Λ^{sx} . Another important feature of Eq. (36) is the absence of the backflow term of the charge current, which usually exists in the nonequilibrium current flow. (See the discussion on the usual Meissner current in the next section.) This is related to the fact that the current induced by a static magnetic field is a dissipationless equilibrium flow. As a result, *the Fermi liquid corrections do not exist in this magnetoelectric coefficient for heavy fermion superconductors, provided that there is no ferromagnetic fluctuation.* This is one of the main results of this paper. In terms of the Kubo formula, the absence of electron correlation effects for \mathcal{K}_{yx} is understood as follows. \mathcal{K}_{yx} is given by the correlation function of the current and spin-density operators. The spin-density vertex is renormalized by electron correlation in the opposite way to the

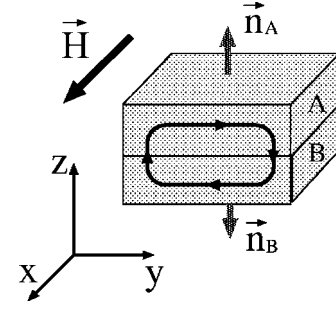


FIG. 2. An experimental setup for the detection of the Zeeman-field-induced supercurrent. The \vec{n} vectors of the two superconducting samples A and B (depicted by the gray arrows) are aligned in the directions $(0,0,1)$ and $(0,0,-1)$, respectively. The in-plane magnetic field \vec{H} is applied in the x direction. The paramagnetic supercurrent circulates in the system as depicted by the black thin arrows.

current vertex, resulting in the cancellation of the mass renormalization factors. The important implication of this result is that the Zeeman-field-induced paramagnetic supercurrent is not suppressed by electron correlation effects in contrast with the usual diamagnetic supercurrent of which the magnitude is much reduced by the large mass enhancement in heavy fermion systems. This property may make the experimental observation of the magnetoelectric effect easier, as discussed in the next section.

V. IMPLICATIONS FOR EXPERIMENTAL OBSERVATIONS

On the basis of the formula (36), we would like to discuss how the Zeeman-field-induced paramagnetic supercurrent is experimentally observed.

When the magnetic field is applied in the x direction, the London equation is modified to

$$\vec{J}_s = -\frac{c}{4\pi\lambda^2} \vec{A} + \mathcal{K}_{yx} (\vec{n} \times \vec{H}_x), \quad (39)$$

where \vec{A} is the vector potential. Since the applied magnetic field always induces both the diamagnetic and the paramagnetic supercurrent in the system with the Rashba spin-orbit interaction, it is important for the experimental observation of this effect to discriminate between these two supercurrents. If one measures currents simply attaching leads to the sample and applying an in-plane magnetic field, the Zeeman-field-induced paramagnetic supercurrent cannot flow in the sample because it generates the Joule heat in the normal metal leads.²⁴ In this case, the magnetoelectric effect is canceled with the nonzero phase gradient of the superconducting order parameter in the equilibrium state.

Here, to highlight the observation of the paramagnetic supercurrent, we consider an experimental setup composed of two superconducting samples joined together as depicted in Fig. 2. The \vec{n} vectors of the sample A and B are, respectively, given by $\vec{n}_A = (0,0,1)$ and $\vec{n}_B = -\vec{n}_A$. The joined surface at the junction is normal to the \vec{n} vectors. The applied magnetic field in the x direction $\vec{H} = (H,0,0)$ gives rise to the paramagnetic supercurrent in the sample A (B) in the direc-

tion $\vec{n}_A \times \vec{H}(-\vec{n}_A \times \vec{H})$. Then, electrons accumulated in the right (left) edge of the sample A (B) transfer to the right (left) edge of the sample B (A) to decrease the chemical potential difference between the samples A and B, resulting in supercurrent flows circulating in the system. The applied magnetic field also induces the Meissner diamagnetic supercurrent. As explained below, the paramagnetic contribution can be discriminated from the diamagnetic current by using the Volovik effect.²⁵

Let us first consider the coefficient of the diamagnetic Meissner supercurrent with the Fermi liquid corrections at zero temperature, which is equal to the Drude weight in the normal state,¹⁴

$$\frac{c}{4\pi\lambda^2} = \frac{e^2}{c} \sum_{p,\tau=\pm 1} v_{p\tau}^{\mu*} J_{p\tau}^{\mu*} \delta(\mu - \varepsilon_{p\tau}^*), \quad (40)$$

where the quasiparticle velocity is $v_{p\tau}^{\mu*} = \partial \varepsilon_{p\tau}^* / \partial p_\mu$, and the charge current is

$$J_{p\tau}^{\mu*} = v_{p\tau}^{\mu*} + \sum_p f_{p\tau,p'\tau'} \delta(\mu - \varepsilon_{p\tau}^*) v_{p'\tau'}^{\mu*}. \quad (41)$$

Here $f_{p\tau,p'\tau'}$ is the interaction between two quasiparticles. The second term of Eq. (41) is the backflow term. In heavy fermion systems, the mass renormalization factor $z_{p\tau}$ and the backflow term in the current $J_{p\tau}^{\mu*}$ give rise to the pronounced reduction of the Meissner coefficient. For example, in CePt₃Si, $z_{p\tau}$ is estimated as $\sim 1/100$.^{6,10} If we assume the spherical Fermi surface, Eq. (40) reduces to $(e^2/c)v_F^* n_s / p_F$. Here v_F^* is the renormalized Fermi velocity, n_s is the superfluid density, and p_F is the Fermi momentum. It should be notified that n_s is renormalized by the backflow effect of $J_{p\tau}^{\mu*}$ and is not equal to the carrier density even at zero temperature. In particular, for heavy fermion systems in which umklapp scattering is expected to be strong, n_s is smaller than the carrier density. In contrast to the diamagnetic Meissner current, the Zeeman-field-induced paramagnetic supercurrent is not influenced by the many-body effects described above, as discussed in the previous section. This difference of electron correlation effects between the diamagnetic and paramagnetic supercurrents can be utilized to detect the magnetoelectric effect.

If the superconducting gap has a nodal structure as is often realized in some heavy-fermion superconductors, the existence of the paramagnetic supercurrent is indirectly observed through the Volovik effect on the single-particle density of states under the applied in-plane magnetic field for $H_{c1} < H < H_{c2}$. Here H_{c1} and H_{c2} are, respectively, the lower and upper critical field. In fact, the recent thermal transport measurements for CePt₃Si supports the existence of the line node in the superconducting state of this system.²³ Applying the semiclassical approximation based upon the Doppler shift effect,²⁵ and assuming a spherical Fermi surface, we calculate the local density of states from the modified London equation (39). In the calculation of \mathcal{K}_{yx} , we use the fact that the vertex correction $\Lambda_{\tau(+)}^{sx}$ is appropriately approximated as $\sim z_{p\tau}^{-1}$ in typical heavy-fermion systems as discussed in Sec. IV, and we expand Eq. (36) in terms of $\alpha p_F / E_F$ up to the lowest order. The result at $T=0$ is

$$\delta D_{\text{loc}}(0) \sim \left| \sqrt{\frac{H}{H_{c2}}} \frac{e^2 v_F^* \Phi_0}{c \xi} \pm \frac{H}{H_{c2}} \frac{e \mu_B \alpha p_F \Phi_0 n_0}{\pi \xi^2 E_F n_s} \right|. \quad (42)$$

Here $\Phi_0 = hc/(2e)$, and n_0 is the density of electrons. E_F is the unrenormalized Fermi energy. The first term on the right-hand side of Eq. (42) is due to the usual Volovik effect, and the second term linearly proportional to the applied magnetic field stems from the Zeeman-energy-induced paramagnetic supercurrent. Thus, the magnetic-field dependence distinguishes between the paramagnetic and diamagnetic currents. The above behavior of the local density of states may be observed by the measurement of the specific-heat coefficient or the thermal conductivity in sufficiently low field regions.^{26–29} In the above expression of $\delta D_{\text{loc}}(0)$, it is seen that the conventional diamagnetic contribution is suppressed by the mass renormalization factor $z_{p\tau}$ which appears through v_F^* , whereas the magnetoelectric contribution is not affected by this correlation effect. It is also noted that the carrier density which enters into the paramagnetic term is not n_s but equal to the electron density n_0 . This is due to the absence of the backflow term in the Zeeman-energy-induced supercurrent. As mentioned before, n_s is affected by the backflow term. For simplicity, we assume that $n_s \approx n_0$ for a while.

In the case of CePt₃Si, according to the measurement of H_{c2} , the coherence length $\xi \sim 8.1 \times 10^{-7}$ cm.⁶ It is a bit difficult to estimate the renormalized Fermi velocity from experimental measurements. Bauer *et al.* obtained $v_F^* \sim 5.29 \times 10^5$ cm/s from the data of dH_{c2}/dT and the specific-heat coefficient, assuming a spherical Fermi surface.⁶ This value of v_F^* is almost of the same order as that obtained by combining the unrenormalized Fermi velocity computed from the LDA method and the mass enhancement factor $z^{-1} \sim 100$ estimated from the specific-heat measurement.^{6,10} According to the LDA band calculations,^{10,30} the spin-orbit splitting is not so small compared to the Fermi energy, and may be approximated as $\alpha p_F / E_F \sim 0.1$. Then, for CePt₃Si, we have

$$\delta D_{\text{loc}}(0) \sim \left| 1.0 \times 10^{-24} \sqrt{\frac{H}{H_{c2}}} \pm 0.48 \times 10^{-24} \frac{H}{H_{c2}} \right|. \quad (43)$$

It is remarkable that the contribution from the paramagnetic supercurrent [the second term of Eq. (43)] is comparable to that from the Meissner supercurrent [the first term of Eq. (43)]. It should be stressed that the feasibility of the experimental observation of Edelstein's magnetoelectric effect is due to the large mass enhancement in the heavy-fermion system, which suppresses strongly the Meissner supercurrent, but in contrast, does not affect the Zeeman-field-induced paramagnetic supercurrent. Moreover, if the superfluid density n_s is reduced by the backflow effect, the Meissner term of Eq. (42) is more suppressed compared with the paramagnetic term, and thus the observation of the magnetoelectric effect may become easier.

VI. SUMMARY AND DISCUSSION

We have investigated electron correlation effects on the magnetoelectric transport phenomena in superconductors

without inversion symmetry. It is found that, in contrast to the Meissner diamagnetic supercurrent which is much reduced by the mass enhancement factor in the absence of translational symmetry, the Zeeman-field-induced paramagnetic supercurrent is not affected by the strong electron correlation provided that ferromagnetic fluctuation is not developed. Because of this remarkable property, the experimental detection of the magnetoelectric effect may be more feasible in heavy-fermion superconductors without inversion symmetry such as CePt₃Si, where the enormous mass enhancement suppresses the magnitude of the Meissner supercurrent, than in conventional metals with moderate effective electron mass. We have proposed the experimental setup for the observation of the magnetoelectric effect in CePt₃Si which utilizes the Volovik effect. It has been also pointed out that in noncentrosymmetric *p* wave superconductors, the coherence effect on the nuclear relaxation rate $1/T_1T$ is similar to that of conventional *s*-wave superconductors.

Finally, we would like to comment on the implication of our results for UIr, which is the recently discovered ferromagnetic superconductor without inversion symmetry.⁷ UIr exhibits superconductivity under high pressure in the vicinity of the phase boundary between ferromagnetic and nonmag-

netic states. The resistivity of this system increases remarkably as the applied pressure approaches the critical value at which the ferromagnetism disappears, indicating the existence of ferromagnetic critical fluctuation. In this case, the magnetoelectric coefficient Eq. (36) may be enhanced by the three-point vertex functions $\Lambda_{\tau(+)}^{xx}$, of which the magnitudes are much increased by ferromagnetic fluctuation, provided that the spin easy axis is taken as the *x* axis. Since the crystal structure of UIr is monoclinic, and does not possess any mirror planes, the Rashba spin-orbit interaction with the \vec{n} vector perpendicular to the spin easy axis should always exist. Thus, the magnetoelectric effect strongly enhanced by ferromagnetic fluctuation may be observed in UIr under an applied magnetic field parallel to the spin easy axis.

ACKNOWLEDGMENTS

The author would like to thank K. Yamada, Y. Matsuda, and H. Ikeda for invaluable discussions. This work was partly supported by a Grant-in-Aid from the Ministry of Education, Science, Sports and Culture, Japan.

-
- ¹L. S. Levitov, Yu. V. Nazarov, and G. M. Eliashberg, *Sov. Phys. JETP* **61**, 133 (1985).
²V. M. Edelstein, *Solid State Commun.* **73**, 233 (1990).
³V. M. Edelstein, *Sov. Phys. JETP* **68**, 1244 (1989).
⁴V. M. Edelstein, *Phys. Rev. Lett.* **75**, 2004 (1995).
⁵S. K. Yip, *Phys. Rev. B* **65**, 144508 (2002).
⁶E. Bauer, G. Hilscher, H. Michor, Ch. Paul, E. W. Scheidt, A. Gribanov, Yu. Seropegin, H. Noël, M. Sigrist, and P. Rogl, *Phys. Rev. Lett.* **92**, 027003 (2004).
⁷T. Akazawa, H. Hidaka, H. Kotegawa, T. Kobayashi, T. Fujiwara, E. Yamamoto, Y. Haga, R. Settai, and Y. Ōnuki, *J. Phys. Soc. Jpn.* **73**, 3129 (2004).
⁸M. Hanawa, J. Yamaura, Y. Muraoka, F. Sakai, and Z. Hiroi, *J. Phys. Chem. Solids* **63**, 1027 (2002).
⁹T. Takeuchi, S. Hashimoto, T. Yasuda, H. Shishido, T. Ueda, M. Yamada, Y. Obiraki, M. Shiimoto, H. Kohara, T. Yamamoto, K. Sugiyama, K. Kindo, T. D. Matsuda, Y. Haga, Y. Aoki, H. Sato, R. Settai, and Y. Ōnuki, *J. Phys.: Condens. Matter* **16**, L333 (2004).
¹⁰S. Hashimoto, T. Yasuda, T. Kubo, H. Shishido, T. Ueda, R. Settai, T. D. Matsuda, Y. Haga, H. Harima, and Y. Ōnuki, *J. Phys.: Condens. Matter* **16**, L287 (2004).
¹¹N. Metoki, K. Kaneko, T. D. Matsuda, A. Galatanu, T. Takeuchi, S. Hashimoto, T. Ueda, R. Settai, Y. Ōnuki, and N. Berngoeft, *J. Phys.: Condens. Matter* **16**, L207 (2004).
¹²M. Yogi, Y. Kitaoka, S. Hashimoto, T. Yasuda, R. Settai, T. D. Matsuda, Y. Haga, Y. Ōnuki, P. Rogl, and E. Bauer, *Phys. Rev. Lett.* **93**, 027003 (2004).
¹³E. I. Rashba, *Sov. Phys. Solid State* **2**, 1109 (1960).
¹⁴A. J. Leggett, *Phys. Rev.* **140**, 1869 (1965); **147**, 119 (1966).
¹⁵A. I. Larkin and A. B. Migdal, *Sov. Phys. JETP* **17**, 1146 (1963).
¹⁶S. Fujimoto, *J. Phys. Soc. Jpn.* **61**, 765 (1992).
¹⁷See, e.g., J. R. Schrieffer, *Theory of Superconductivity* (Addison Wesley, Reading, MA, 1983).
¹⁸L. P. Gor'kov and E. I. Rashba, *Phys. Rev. Lett.* **87**, 037004 (2001).
¹⁹P. A. Frigeri, D. F. Agterberg, A. Koga, and M. Sigrist, *Phys. Rev. Lett.* **92**, 097001 (2004).
²⁰I. A. Sergienko and S. H. Curnoe, *Phys. Rev. B* **70**, 214510 (2004).
²¹J. M. Luttinger and J. C. Ward, *Phys. Rev.* **118**, 1417 (1960).
²²J. M. Luttinger, *Phys. Rev.* **119**, 1153 (1960).
²³K. Izawa, Y. Kasahara, Y. Matsuda, K. Behnia, T. Yasuda, R. Settai, and Y. Ōnuki, *Phys. Rev. Lett.* **94**, 197002 (2005).
²⁴If the attached leads are made of superconductors with the transition temperature higher than that of the sample and the same pairing symmetry as that of $\Delta_s(p)$ and $\Delta_l(p)$, the Zeeman-field-induced supercurrent can flow in the system. Note that the tunneling amplitude between the leads and the noncentrosymmetric superconductor does not depend on the symmetric properties of the \vec{d} vector of the gap function (12), $\vec{t}_p \times \vec{n}$, as pointed out by I. A. Sergienko and S. H. Curnoe, in Ref. 18. The observation of the magnetoelectric effect may be possible also in this case, as discussed in Sec. V.
²⁵G. E. Volovik, *JETP Lett.* **58**, 469 (1993).
²⁶C. Kübert and P. J. Hirschfeld, *Phys. Rev. Lett.* **80**, 4963 (1998).
²⁷M. Franz, *Phys. Rev. Lett.* **82**, 1760 (1999).
²⁸I. Vekhter and A. Houghton, *Phys. Rev. Lett.* **83**, 4626 (1999).
²⁹M. Chiao, R. W. Hill, C. Lupien, B. Popic, R. Gagnon, and L. Taillefer, *Phys. Rev. Lett.* **82**, 2943 (1999).
³⁰K. V. Samokhin, E. S. Zijlstra, and S. K. Bose, *Phys. Rev. B* **69**, 094514 (2004).